Materials Science Forum Vol. 802 (2014) pp 421-426
Online available since 2014/Dec/31 at www.scientific.net

doi:10.4028/www.scientific.net/MSF.802.421

Submitted: 01.10.2014
Accepted: 06.10.2014

Microstructure and Electrochemical Characteristics of LaPrMgAlMnCoNi Hydrogen Storage Alloys for Nickel-Metal Hydride Batteries

Lia Maria Carlotti Zarpelon[a] and Rubens Nunes Faria Jr.[b]

Instituto de Pesquisas Energéticas e Nucleares, IPEN-CNEN/SP, São Paulo, Brazil

[a]email: zarpelon@ipen.br, [b]email: rfaria@ipen.br

Keywords: hydrogen storage alloys, rare earth alloys, metal hydrides, electrochemical properties

Abstract. The effect of the substitution of La with Pr on the microstructure and some electrochemical properties of $La_{0.7-x}Pr_xMg_{0.3}Al_{0.3}Mn_{0.4}Co_{0.5}Ni_{3.8}$ (x=0.0, 0.1, 0.3, 0.5, and 0.7) ingot alloys as powder electrode was studied in this paper. XDR and SEM (+EDX) analyses revealed that the as-cast alloys consist mainly of similar $LaNi_5$ and $(La,Pr)Mg_2Ni_9$ phases. With the increase in Pr content, both the relative abundance of the phases and microstructure changed. The electrochemical studies showed that the maximum discharge capacity decreased with the increase in Pr content. For the alloy without Pr, the self-discharge studies revealed a major stability of the hydride until the first 984 hours (41 days) of the charge/discharge cycles. The high-rate dischargeability of this alloy electrode showed the best result HRD=88% at a discharge current density of I_d=250 mA/g.

Introduction

Nickel-metal hydride (Ni/MH) batteries are based on hydrogen storage alloy electrode and nowadays are commercially important rechargeable batteries for both consumer and industrial applications [1-6]. In this context, they are considered as the preferred rechargeable batteries for portable power tools, electric vehicles (EVs), hybrid electric vehicles (HEVs), and plug-in hybrid electric vehicles (PHEVs) because of the following major advantages: (a) high specific-power or power density, (b) flexible cell sizes from 30 mAh–250 Ah, (c) safe operation at high voltage (320+ V), (d) easy application to series and series/parallel strings, (e) safety in charge and discharge, including tolerance to abusive overcharge and overdischarge, (f) maintenance free, (g) excellent thermal properties, (h) simple and inexpensive charging and electronic control circuits, (i) environmentally compatibility and recyclable materials. Rare earth-Mg–Ni-based hydrogen storage alloys have been developed in the last decade as the most promising next-generation negative electrode materials for high energy and high power Ni/MH batteries. Praseodymium has been cited as rare earth element with role in improving the cyclic stability associated with enhancing the electrochemical kinetics, but decreasing the maximum discharge capacity [2]. High-rate dischargeability (HRD) is one of the main factors that represent the kinetic property of the hydrogen storage alloy. Self-discharge, one of the major parameters for estimating a battery performance, is mainly ascribed to the hydrogen desorption from the hydride electrodes which is related to the stability of the hydrides. Thereby the gradual increase of the stability of the hydrides makes the self-discharge of the alloy electrodes decrease [5,6]. The aim of this work is to investigate the influence of the substitution of La with Pr on the $La_{0.7-x}Pr_xMg_{0.3}Al_{0.3}Mn_{0.4}Co_{0.5}Ni_{3.8}$ (x = 0, 0.1, 0.3, 0.5, and 0.7) as-cast hydrogen storage alloys. Microstructural characteristics, self-discharge and high-rate dischargeability of these materials have been studied and reported.

Experimental

The alloys were prepared in 5 kg batches melted in an induction heating furnace and cast in a water-cooled copper mold. The microstructures of these alloys were examined using a scanning electron microscopy (SEM) with energy dispersive X-ray (EDX) analysis facilities. The chemical

compositions of these alloys, a general view of their as-cast microstructures, the X-ray diffraction (XRD) patterns, and a detailed phase analyses have all been reported in a previous papers [3,4].

The hydrogen storage pellet-type alloy electrodes were prepared by cold pressing a mixture of 0.1 g of the active alloy powders (mechanically crushed in air and ground into powders of 270 mesh size (<53 μm)) and teflonized carbon (Vulcan XC-72R with 33 wt.% PTFE (polytetrafluoroethylene)) in weight ratio 1:1 on both sides of a nickel screen (d=10 mm). The electrochemical charge/discharge cycling tests were performed on an Arbin BT2000 battery tester at room temperature. Electrochemical measurements were carried out in an open tri-electrode cell consisting of a working electrode (pellet-type alloy electrode), a Pt wire (d=0.5 mm; l=300 mm) counter electrode and a reference electrode of Hg/HgO, in a 6 M KOH electrolyte solution. Each electrode was charged at 100 mA/g for 5 h and then discharged at 50 mA/g to the cut-off potential of -0.6 V versus the Hg/HgO reference electrode.

The self-discharge rate (SDR) of the alloy electrode was evaluated using the formula

$$SDR = 1 - \frac{2C_b}{C_a + C_c} \times 100\% \quad (1)$$

where C_b is the discharge capacity after laying for 24 h (open circuit), and C_a and C_c are the discharge capacities tested before and after C_b, respectively [5]. The tests were carried out at a charge current density of 100 mA/g and at a discharge current density of 200 mA/g.

For investigating high-rate dischargeability (HRD), the discharge capacities of the alloy electrode at various discharge current densities were measured. The HRD is defined and calculated according to the formula

$$HRD = \frac{C_d}{C_d + C_{60}} \times 100\% \quad (2)$$

where C_d is the discharge capacity at the discharge current density I_d, C_{60} is the residual discharge capacity at the discharge current density I_d=60 mA/g after the alloy electrode has been fully discharged at larger discharge current density (I_d) [5,6].

Results and Discussion

Fig.1 (a) and (b) shows respectively the SEM micrographs of the $La_{0.7-x}Pr_xMg_{0.3}Al_{0.3}Mn_{0.4}Co_{0.5}Ni_{3.8}$ (x=0.0 and 0.7) as-cast alloys. The alloy without Pr shows a coarse grain structure, whereas that the total substitution of La with Pr reveals a fine grain structure. It can be seen that this substitution resulted in a marked change in the grain structure of the cast alloys. Phase analyses revealed that the $La_{0.7-x}Pr_xMg_{0.3}Al_{0.3}Mn_{0.4}Co_{0.5}Ni_{3.8}$ (x = 0.0, 0.1, 0.3, 0.5, and 0.7) as-cast alloys are composed of a matrix phase (M), a gray phase (G) and a dark phase (D). The M phase matched a similar $LaNi_5$ phase and the G phase matched a similar $REMg_2Ni_9$ phase (RE=La,Pr). The dark phase was very heterogeneous, contained Al, Mn and Co in significant amounts but with a relative abundance much smaller than that of the matrix phase and of that of the gray phase.

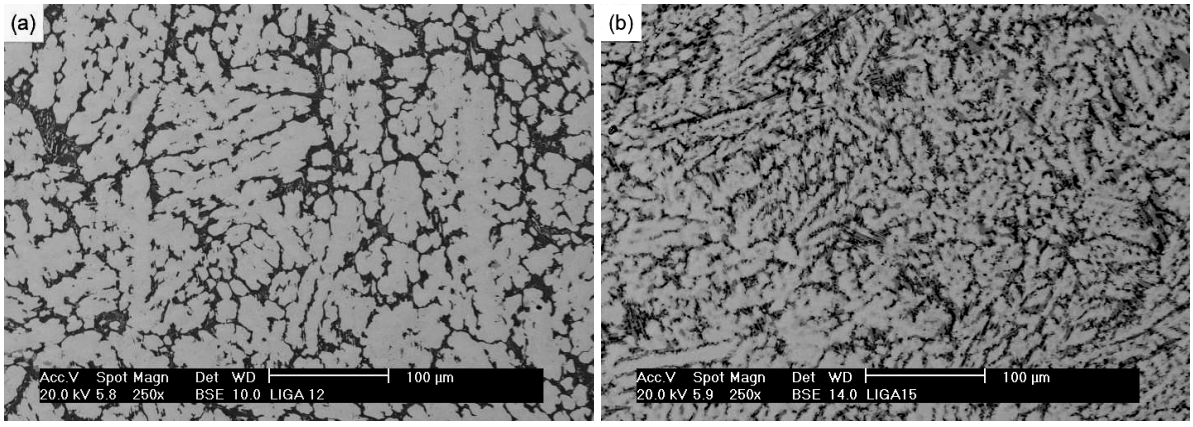

Fig. 1. SEM images of $La_{0.7-x}Pr_xMg_{0.3}Al_{0.3}Mn_{0.4}Co_{0.5}Ni_{3.8}$ as-cast alloys (a) x=0.0 and (b) x=0.7.

Fig. 2 shows the discharge capacity characteristics of the alloys electrodes with cycling. The highest measured value of discharge capacity was ~193 mAh/g and this could be attributed to superficial oxide formation during the preparation of the electrodes in air [7]. It can be seen that the electrodes can be easily activated within 2 cycles. The highest discharge capacity values were obtained for the Pr free alloy (maximum of 192.8 mAh/g) and to the $La_{0.6}Pr_{0.1}Mg_{0.3}Al_{0.3}Mn_{0.4}Co_{0.5}Ni_{3.8}$ alloy (maximum of 159 mAh/g). A significant diminishing on the maximum discharge capacity (~137 mAh/g) was observed for the $La_{0.7-x}Pr_xMg_{0.3}Al_{0.3}Mn_{0.4}Co_{0.5}Ni_{3.8}$ (x=0.3) alloy. A dramatic reduction in this property was verified for the alloys with higher Pr content. Thus, the increasing the Pr content on the alloys visibly decreased the discharge capacity of the negative electrodes. Microstructure observations showed that the increasing Pr content on the alloys diminished the amount of the similar $LaNi_5$ phase.

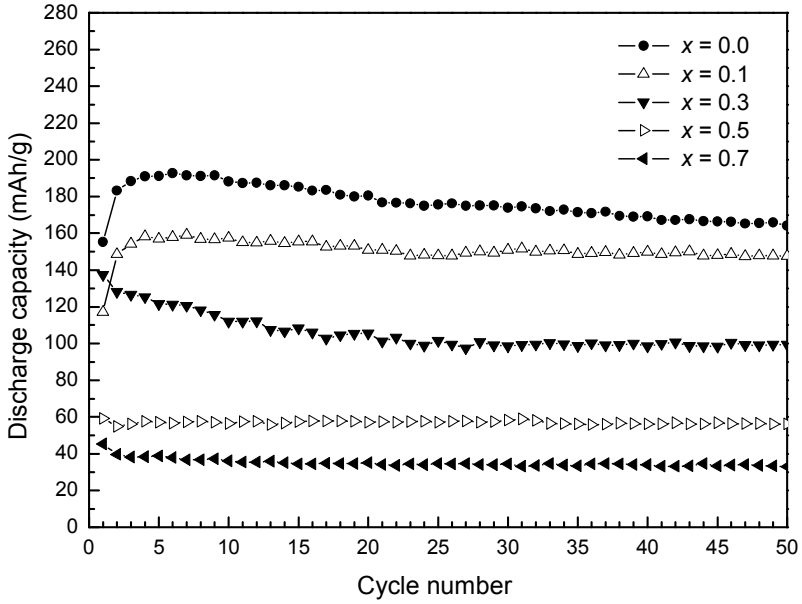

Fig. 2. Discharge capacity of $La_{0.7-x}Pr_xMg_{0.3}Al_{0.3}Mn_{0.4}Co_{0.5}Ni_{3.8}$ as-cast alloy electrodes *vs.* cycle number.

Therefore, comparatively, this phase would favor the discharge capacity of the electrodes for the as-cast condition of the studied alloys. This influence of the chemical composition and phase abundance on the electrochemical characteristics of the alloys is in agreement to previous studies [6,8,9]. The microstructure refining of the alloys with the increasing substitution of La with Pr also proved to be detrimental to the discharge capacity of the negative electrodes. The overall discharge

capacities of the present $La_{0.7-x}Pr_xMg_{0.3}Al_{0.3}Mn_{0.4}Co_{0.5}Ni_{3.8}$ (x=0.0-0.7) as-cast alloys were inferior to those obtained with a composition of $La_{0.7-x}Pr_xMg_{0.3}Al_{0.2}Mn_{0.1}Co_{0.75}Ni_{2.45}$ (x=0.00-0.30) [6], with a composition $La_{0.65-x}Pr_xNd_{0.12}Mg_{0.23}Al_{0.1}Ni_{3.4}$ (x=0.00–0.20) [8], and with a composition $La_{0.55}Pr_{0.05}Nd_{0.15}Mg_{0.25}Ni_{3.5}$ [10], all in the range of about 360 mAh/g. The discrepancies can be attributed to the alloy preparation method, testing conditions and to the considerable differences in the alloys compositions.

The self-discharge rate of the $La_{0,7}Mg_{0,3}Al_{0,3}Mn_{0,4}Co_{0,5}Ni_{3,8}$ (x=0.0) alloy electrode is showed in Fig. 3. The top x axis shows the cycling time corresponding to the carried out SDR measured.

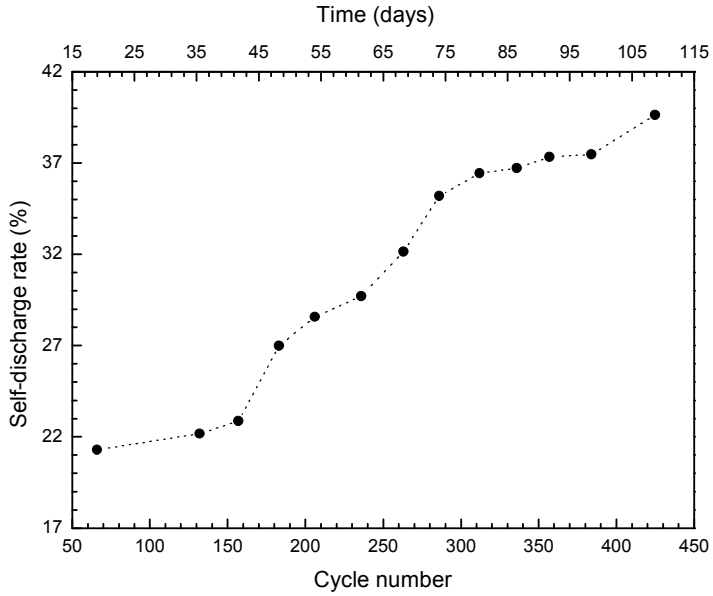

Fig. 3. Self-discharge rate of $La_{0,7}Mg_{0,3}Al_{0,3}Mn_{0,4}Co_{0,5}Ni_{3,8}$ alloy electrode vs. cycle number.

It can be seen that there was a slight increase between the first SDR measurement and the third (21.3 to 22.9 %) which indicated that until the first forty-one days of charge/discharge cycling tests (between cycles 66 and 157), the stability of the formed hydride has been maintained. Soon after the hydride stability diminished considerably reaching the SDR value of approximately 27% in the cycle number 183 or after 49 days of cycling. The electrode self-discharge increased gradually reaching 39,6 % in 109 days or 425 cycles.

Fig.4 shows the HRD of $La_{0,7}Mg_{0,3}Al_{0,3}Mn_{0,4}Co_{0,5}Ni_{3,8}$ alloy electrode at different discharge current densities, and Fig. 5 shows the correspondent discharge profiles. It can be noted that the HRD of the alloy electrode decreases with the increase of discharge current density. The best result was verified at I_d=250 mA/g, with a HRD value of about 88%. This result is very close to that reported to the $La_{0.4}Pr_{0.3}Mg_{0.3}Al_{0.2}Mn_{0.1}Co_{0.75}Ni_{2.45}$ alloy (HRD ~90%) tested at the same current density [6].

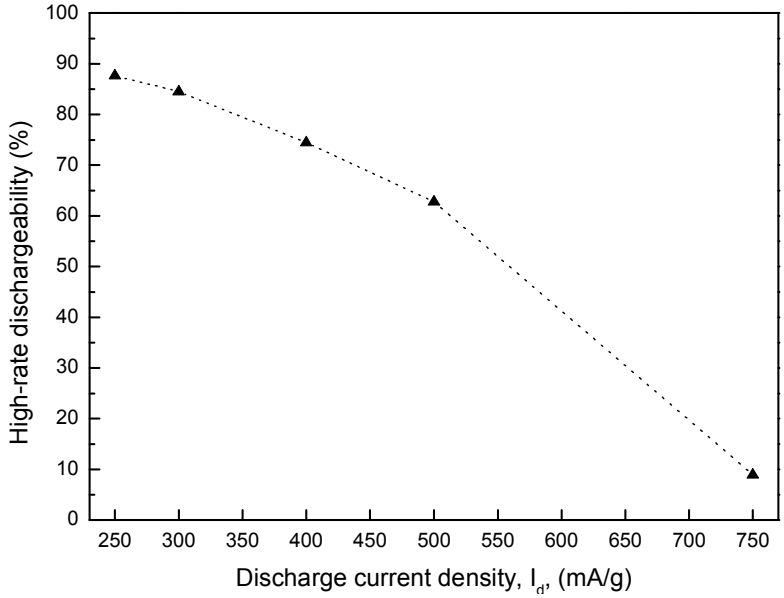

Fig. 4. HRD of the $La_{0,7}Mg_{0,3}Al_{0,3}Mn_{0,4}Co_{0,5}Ni_{3,8}$ alloy electrode.

The following HRD make evident the increasing reduction on the electrode kinetics and the corresponding diminution on the electrode discharge time with higher current densities, as showed in Fig. 5. As it is generally accepted that the HRD of a MH electrode is mainly determined by the charge-transfer process occurring at the metal/electrolyte interface and/or the hydrogen diffusion process in the bulk of alloy [5], certainly these processes influenced the behavior noticed in this study.

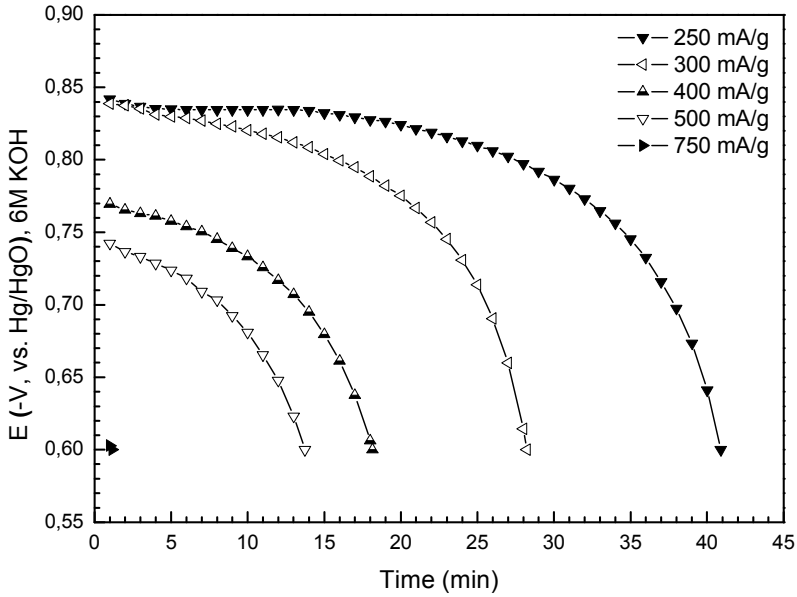

Fig. 5. Discharge profiles of the $La_{0,7}Mg_{0,3}Al_{0,3}Mn_{0,4}Co_{0,5}Ni_{3,8}$ alloy electrode at different discharge current densities.

Conclusions

Substitution of La with Pr in the LaPrMgAlMnCoNi as-cast alloys changed the grain structure from coarse to fine columnar characteristics. This change and the decrease in the presence of a similar $LaNi_5$ phase were associated to the decrease in the discharges capacities of the alloy electrodes with Pr substitution. The cast $La_{0.7}Mg_{0.3}Al_{0.3}Mn_{0.4}Co_{0.5}Ni_{3.8}$ alloy electrode exhibited the with highest discharge capacity. The stability of the formed hydride on this alloy was greater on the

first 984 hours (41 days) of cycling and the best kinetic response (HRD=88%) has been obtained with a discharge current density of 250 mA/g.

Acknowledgements

The authors wish to thank FAPESP and IPEN-CNEN/SP for the financial support and infrastructure made available to carry out this investigation.

References

[1] D. Linden, T.B. Reddy: ***Handbook of Batteries***. (Mc Graw-Hill, New York, 2002).
[2] Y. Liu, H. Pan, M. Gao, Q. Wang: J. Mater. Chem. Vol. 21 (2011), p. 4743.
[3] L.M.C. Zarpelon, E. Galego, H. Takiishi, R.N. Faria: Mater. Res. Vol. 11 (2008), p. 17.
[4] E.P. Banczek, L.M.C. Zarpelon, R.N. Faria, I. Costa: J. Alloys Compd. Vol. 479 (2009), p. 342.
[5] S. Yang, S. Han, J. Song, Y. Li: J. Rare Earths Vol. 29 (2011), p. 692.
[6] H. Pan, S. Ma, J. Shen, J. Tan, J. Deng, M. Gao: Int. J. Hydrogen Energy Vol. 32 (2007), p. 2949.
[7] D.J. Cuscueta, M. Melnichuk, H.A. Peretti, H.R. Salva, A.A. Ghilarducci: Int. J. Hydrogen Energy Vol. 33 (2008), p. 3566.
[8] H. Yan, F. Kong, W. Xiong, B. Li, J. Li: J. Rare Earths Vol. 27 (2009), p. 244.
[9] Y. Li, D. Han, S. Han, X. Zhu, L. Hu, Z. Zhang, Y. Liu: Int. J. Hydrogen Energy Vol. 34 (2009), p. 1399.
[10] M. Qin, Z. Lan, Y. Ding, K. Xiong, Y. Liu, J. Guo: J. Rare Earths Vol. 30 (2012), p. 222.

Advanced Powder Technology IX
10.4028/www.scientific.net/MSF.802

Microstructure and Electrochemical Characteristics of LaPrMgAlMnCoNi Hydrogen Storage Alloys for Nickel-Metal Hydride Batteries
10.4028/www.scientific.net/MSF.802.421

DOI References
[2] Y. Liu, H. Pan, M. Gao, Q. Wang: J. Mater. Chem. Vol. 21 (2011), p.4743.
http://dx.doi.org/10.1039/c0jm01921f
[3] L.M.C. Zarpelon, E. Galego, H. Takiishi, R.N. Faria: Mater. Res. Vol. 11 (2008), p.17.
http://dx.doi.org/10.1590/S1516-14392008000100004
[4] E.P. Banczek, L.M.C. Zarpelon, R.N. Faria, I. Costa: J. Alloys Compd. Vol. 479 (2009), p.342.
http://dx.doi.org/10.1016/j.jallcom.2008.12.075
[5] S. Yang, S. Han, J. Song, Y. Li: J. Rare Earths Vol. 29 (2011), p.692.
http://dx.doi.org/10.1016/S1002-0721(10)60524-8
[6] H. Pan, S. Ma, J. Shen, J. Tan, J. Deng, M. Gao: Int. J. Hydrogen Energy Vol. 32 (2007), p.2949.
http://dx.doi.org/10.1016/j.ijhydene.2006.12.023
[7] D.J. Cuscueta, M. Melnichuk, H.A. Peretti, H.R. Salva, A.A. Ghilarducci: Int. J. Hydrogen Energy Vol. 33 (2008), p.3566.
http://dx.doi.org/10.1016/j.ijhydene.2007.12.013
[8] H. Yan, F. Kong, W. Xiong, B. Li, J. Li: J. Rare Earths Vol. 27 (2009), p.244.
http://dx.doi.org/10.1016/S1002-0721(08)60228-8
[9] Y. Li, D. Han, S. Han, X. Zhu, L. Hu, Z. Zhang, Y. Liu: Int. J. Hydrogen Energy Vol. 34 (2009), p.1399.
http://dx.doi.org/10.1016/j.ijhydene.2008.11.049
[10] M. Qin, Z. Lan, Y. Ding, K. Xiong, Y. Liu, J. Guo: J. Rare Earths Vol. 30 (2012), p.222.
http://dx.doi.org/10.1016/S1002-0721(12)60027-1